Japanese Journal of Applied Physics **55**, 07KF11 (2016)
http://doi.org/10.7567/JJAP.55.07KF11

REGULAR PAPER

Accurate evaluation of viscoelasticity of radial artery wall during flow-mediated dilation in ultrasound measurement

Yasumasa Sakai[1], Hirofumi Taki[2,1], and Hiroshi Kanai[1,2*]

[1]*Graduate School of Engineering, Tohoku University, Sendai 980-8579, Japan*
[2]*Graduate School of Biomedical Engineering, Tohoku University, Sendai 980-8579, Japan*

*E-mail: kanai@ecei.tohoku.ac.jp

Received November 13, 2015; accepted March 25, 2016; published online June 16, 2016

In our previous study, the viscoelasticity of the radial artery wall was estimated to diagnose endothelial dysfunction using a high-frequency (22 MHz) ultrasound device. In the present study, we employed a commercial ultrasound device (7.5 MHz) and estimated the viscoelasticity using arterial pressure and diameter, both of which were measured at the same position. In a phantom experiment, the proposed method successfully estimated the elasticity and viscosity of the phantom with errors of 1.8 and 30.3%, respectively. In an in vivo measurement, the transient change in the viscoelasticity was measured for three healthy subjects during flow-mediated dilation (FMD). The proposed method revealed the softening of the arterial wall originating from the FMD reaction within 100 s after avascularization. These results indicate the high performance of the proposed method in evaluating vascular endothelial function just after avascularization, where the function is difficult to be estimated by a conventional FMD measurement.

1. Introduction

Cardiovascular disease is a major cause of death in Japan, and atherosclerosis is one of the main causes of cardiovascular disease. As a method for the diagnosis of atherosclerosis, there are several techniques such as intravascular ultrasound and diagnosis by X-ray imaging. However, these techniques are unsuitable for repeated tests because of their invasiveness and radiation exposure. As noninvasive diagnostic methods for atherosclerosis, Wetter and Kenner[1)] and McDonald[2)] proposed an index of pulse wave velocity (PWV), and Weitz et al.[3)] proposed an ankle brachial index (ABI). However, these indices are intended to diagnose advanced lesions, not those prior to vascular endothelial dysfunction. In an early stage of atherosclerosis, it is considered that vascular endothelial function is reduced before the appearance of plaques and that the reduction of the endothelial function should still be reversible.[4,5)] Therefore, for the early diagnosis and treatment of atherosclerosis, it is important to develop a noninvasive diagnostic method to evaluate vascular endothelial function.

Endothelial cells react to the shear stress caused by blood flow and produce nitric oxide (NO),[6)] which is a vasodepressor material that stimulates the vessel wall to relax.[7)] This function is important for maintaining the homeostasis of the vascular system. For the evaluation of vascular endothelial function, there is a conventional technique for measuring the transient change in the inner diameter of the brachial artery caused by flow-mediated dilation (FMD) after the release of avascularization.[8–10)] However, this method cannot be used to directly evaluate the mechanical properties (viscoelasticity) of the radial artery wall and it is difficult to diagnose the endothelial function because the rate of diameter change is low, at most about 6% in healthy subjects.[11,12)]

For a more accurate evaluation of the endothelial function, our group has focused on the fact that the change in diameter depends on the mechanical properties of the vessel, and we have measured the transient change in viscoelasticity during FMD with respect to arterial pressure and wall thickness at the same position.[13–18)] However, the viscoelasticity estimated by the employed method had a large variance because it is difficult to measure the minute change in thickness of the radial artery wall, i.e., several micrometers. Furthermore, the method employed a high-frequency (22 MHz) ultrasound device with a single beam, which was much different from a commercial ultrasound diagnostic apparatus. To solve these problems, in the present study, we employed a commercial ultrasound device with a center frequency of 7.5 MHz and measured the change in the diameter of a radial artery, about 100 μm, from which the viscoelasticity of the radial artery wall was estimated. Moreover, in order to measure the changes in the diameter and pressure of the radial artery at the same position, two pressure sensors were employed to correct the time delay due to the pulse wave propagation. After evaluating the accuracy of the proposed method in the estimation of the incremental viscoelasticity of a silicone tube phantom, the proposed method was applied to three healthy subjects to measure the changes in diameter and viscoelasticity during FMD.

2. Methods

2.1 Measurement of arterial pressure and diameter

For the noninvasive evaluation of the elasticity of the artery or soft tissue, some methods have been developed recently.[19,20)] On the other hand, for the noninvasive characterization of viscoelasticity, there have been several methods based on the hysteresis property between the force and the displacement,[21)] and based on the dispersion of shear wave propagation velocity.[22)] In the present study, for the measurement of viscoelasticity in the radial artery wall, changes in thickness and pressure were simultaneously measured. In our previous study, the change in thickness was measured using high-frequency ultrasound transmission with a center frequency of 22 MHz. However, when using a commercial transcutaneous ultrasound device with a center frequency of 7.5 MHz, it was difficult to accurately measure the change in the thickness of the radial artery wall. Alternatively, the change in the diameter of the radial artery was measured to estimate the viscoelasticity of the radial artery.

For the measurement of the pressure at the same point as that for the change in diameter using ultrasound, as shown in Fig. 1, the arterial blood pressure waveforms $p_A(t)$ and $p_B(t)$

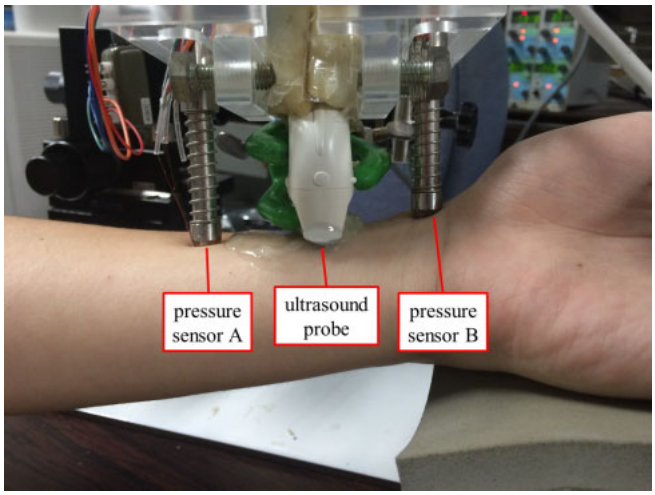

Fig. 1. (Color online) Device for in vivo measurement of viscoelasticity for the radial artery.

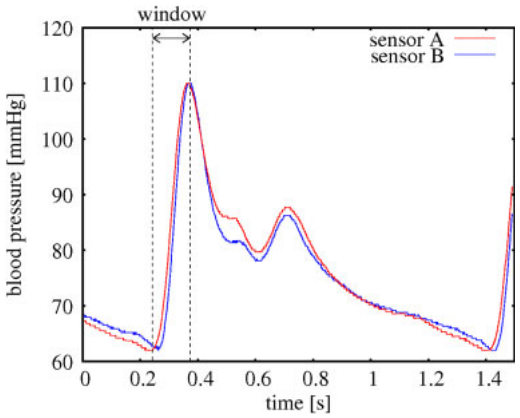

Fig. 2. (Color online) Blood pressures measured by two pressure sensors. The correlation window was set between the two dotted lines.

at two points on the left radial artery were simultaneously measured using two pressure sensors. The time delay τ from $p_A(t)$ to $p_B(t)$ was determined by maximizing the cross-correlation function[23] as

$$\hat{\tau} = \arg\max_{\tau} r_{AB}(\tau), \tag{1}$$

$$r_{AB}(\tau) = \frac{1}{N\sigma_A\sigma_B}\left[\sum_{n=0}^{N-1}(p_A(n\Delta t) - \overline{p_A})(p_B(n\Delta t + \tau) - \overline{p_B})\right], \tag{2}$$

where (σ_A, σ_B) and $(\overline{p_A}, \overline{p_B})$ show the standard deviations and averages of blood pressure waveforms, respectively. As shown in Fig. 2, the window of cross-correlation function was set from the onset of the rise of blood pressure to the peak time of its waveform in order to eliminate the effect of the reflection from the vascular periphery.

In the present study, we assume that the PWV and the pressure waveform between two pressure sensors are constant. Under this condition, the pressure waveform $p_1(t)$ at the position of the ultrasound probe located at the center of two pressure sensors was estimated by compensation for the delay time from the position of the ultrasound probe to that of the pressure sensor B:

$$\widehat{p_1(t)} = p_B\left(t - \frac{\hat{\tau}}{2}\right). \tag{3}$$

Therefore, the pressure $p_1(t)$ could be measured at the same position as that for the measurement of diameter $D(t)$ by the ultrasound probe.

The pressure measured by the pressure sensor reflects the blood pressure in the radial artery. We assume that the maximum and minimum blood pressures in the left radial artery are the same as those in the right radial artery. The blood pressure in the right radial artery was measured using a sphygmomanometer, which was employed to calibrate the pressure waveform measured by the pressure sensor on the left radial artery.

The arterial diameter during a heartbeat was measured using a 7.5 MHz ultrasound probe. The change in arterial diameter was calculated by applying the phased-tracking method[24–27] to the receive RF signals. By this method, a minute displacement is estimated by calculating the phase shift due to the displacement of a target as follows. The received ultrasound pulse has a phase delay, $\theta(t)$, corresponding to the path length. The phase shift, $\Delta\theta(t) = \theta(t+T) - \theta(t)$, is estimated from two consecutive echoes. From the phase shift, the velocity of the target at the time $t + T/2$ is given by

$$v\left(t + \frac{T}{2}\right) = -\frac{c}{2\omega_0}\frac{\Delta\theta(t)}{T}, \tag{4}$$

where T is the pulse repetition interval, and ω_0 and c are the central angular frequency of the ultrasound wave and the speed of sound, respectively. The speed of sound in the tissue is assumed to be 1,540 m/s. The change in diameter, $D(t)$, is obtained by the integration of the difference between the velocity waveforms for the anterior and posterior walls.

2.2 Viscoelasticity estimation

By assuming that the viscoelasticity of the artery wall follows the Voigt model,[28] we estimate the stiffness parameter β and viscosity parameter η from the following equation of the pulse pressure with respect to arterial pressure and diameter:[29]

$$\ln\left[\frac{\widehat{p_1(t)}}{p_{min}}\right] = \beta\varepsilon_1(t) + \eta\frac{d}{dt}\varepsilon_1(t), \tag{5}$$

where $\widehat{p_1(t)}$ is the modeled blood pressure and $\varepsilon_1(t)$ denotes the strain of the diameter. The unit of the viscosity parameter η is second. The viscoelastic constants β and η are estimated by applying the least-squares method to minimize the difference between the measured and modeled arterial pressure waveforms as

$$\alpha = E_t[|\ln p_1(t) - \ln\widehat{p_1(t)}|^2], \tag{6}$$

where $E_t[\cdot]$ denotes the averaging operation with respect to time during a single heartbeat. To suppress noise components, we examined the spatially averaged arterial diameter and viscoelasticity by setting three beams around the center of the radial artery.

2.3 Experimental setting in the phantom experiment

In the present study, the feasibility of the proposed method was validated using a cylindrical phantom made of silicone

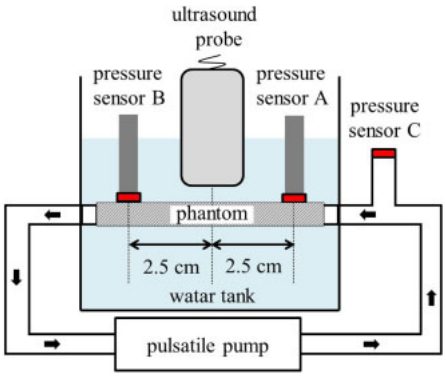

Fig. 3. (Color online) Basic experimental system.

rubber that contained graphite powder as scatterers. Pulsatile flow was used to induce a pulsatile change in internal pressure. Incremental viscoelasticity was estimated from the relationship between pressure and diameter shown by

$$\frac{D_{\min}}{2h}\widehat{P}_2(t) = E_{\text{inc}}\varepsilon_2(t) + \eta_{\text{inc}}\frac{d}{dt}\varepsilon_2(t), \tag{7}$$

where $\widehat{P}_2(t)$ is the model pulse pressure, and ε_2, E_{inc}, η_{inc}, and h are the strain of diameter, incremental elasticity, incremental viscosity, and wall thickness, respectively. The unit of the incremental viscosity η_{inc} is Pascal-second. The incremental viscoelasticity (E_{inc} and η_{inc}) was estimated by the least-squares method with the minimization of the mean squared difference.

Internal pressure waveforms and PWV were measured with two pressure sensors (Kyowa PS-1KC) located 50 mm apart, as shown in Fig. 3. In the in vivo experiment, the pressure waveforms measured using pressure sensors A and B were calibrated by the direct measurement of the water pressure using sensor C. The change in the inner diameter of the phantom was measured using an ultrasound diagnostic device (Hitachi-Aloka ProSound F75) with a 7.5 MHz linear array probe (Hitachi-Aloka UST-5415) placed at the center of the two pressure sensors. The sampling frequency of the ultrasound signal was 40.0 MHz and the frame rate was 252 Hz. Furthermore, the propagation time between the pressure waveforms measured by sensors A and B was estimated by using the cross-correlation function, and PWV was estimated from the relationship between distance and propagation time. Finally, as shown in Eq. (2), the propagation time from the pressure sensor to the ultrasound probe was corrected using this PWV.

2.4 Experimental setting in vivo

In this study, the left radial arteries of three healthy subjects (22–23 years old) were measured. In the in vivo experiment, the same ultrasound-data acquisition setting as that in the phantom study was used, the two pressure sensors being located 74 mm apart. Blood pressure waveforms were acquired at the sampling frequency of 1.0 Hz in the left radial artery. In addition, the blood pressure waveforms were calibrated by systolic and diastolic blood pressures measured with a sphygmomanometer in the right radial artery 5 min after recirculation, because there should have been a small difference between the right and left arterial pressures at the time. The transient changes in diameter and viscoelasticity during FMD were measured. This measurement was repeated every 20 s for 3 min at rest before avascularization and about every 10 s for 5 min after recirculation. Although some methods have been proposed to automatically determine the boundaries of the arterial wall from the received RF signals,[30] in the present study, the lumen-intima boundaries for the anterior and posterior walls were determined from the local maxima of the envelope signal of the received RF signal.

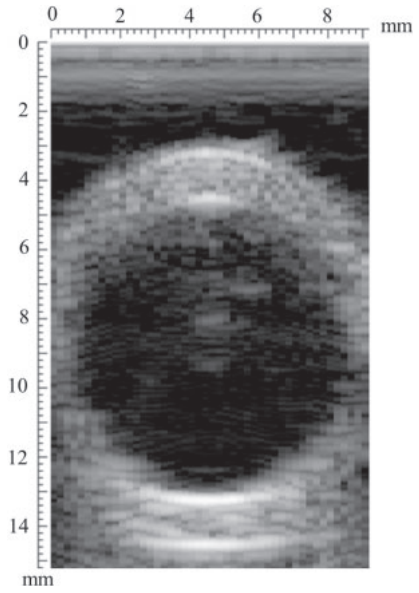

Fig. 4. B-mode image of silicone tube.

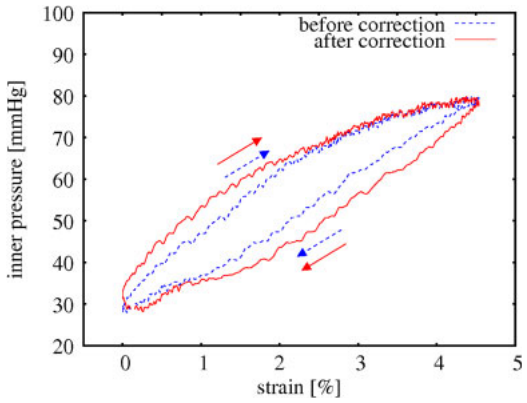

Fig. 5. (Color online) Relationships between diameter and pressure before and after correction of the propagation time.

3. Results

3.1 Results of the basic experiment using vessel phantom

Figure 4 shows a B-mode image of the vessel phantom. The PWV from pressure sensors A to B was estimated. The mean PWV using four measurements was 1.83 m/s, and the propagation time delay between pressure sensor A and the ultrasound probe was corrected using the estimated PWV. Figure 5 shows the relationships between the diameter of the phantom and the pressure before and after the correction of the propagation time delay of the pulse wave.

Figure 6 shows the mean and standard deviation of the incremental viscoelasticity by using three beams near the center of the phantom tube in four measurements. In the

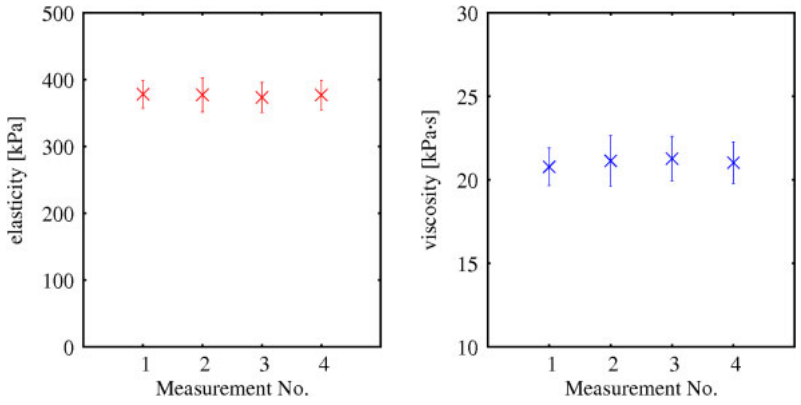

Fig. 6. (Color online) Measured viscoelasticity of phantom in basic experiment using phantom.

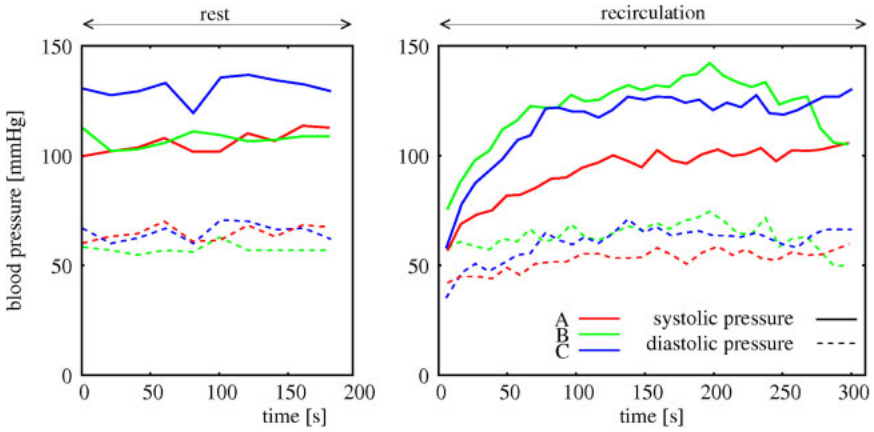

Fig. 7. (Color online) Transient changes in systolic (solid lines, p_s) and diastolic (dot lines, p_d) blood pressures during FMD for three healthy subjects.

ultrasound measurement, the measured mean incremental elasticity and viscosity were 376.5 kPa and 21.1 kPa·s, respectively. The deviations of elasticity and viscosity are 22.6 kPa and 1.3 kPa·s, respectively. This shows that the proposed method had a variance smaller than that of our previous study, where the deviations of elasticity and viscosity were about 130.0 kPa and 2.3 kPa·s, respectively.

To evaluate the accuracy of the proposed method, the viscoelasticity of the phantom was also measured using a tensile tester (Shimadzu Autograph AG-X). The estimated elastic and viscosity moduli of the phantom were 383.5 kPa and 27.5 kPa·s, respectively. Thus, the estimation errors of the elasticity and viscosity were 1.9 and 30.3%, respectively.

3.2 Results of the in vivo experiment

Figure 7 shows the transient changes in systolic and diastolic blood pressures during FMD. The pulse pressure estimated by the proposed method largely decreased just after avascularization.

Figure 8 shows the relationships between diameter and pressure in the radial artery before and after correction using the propagation time and the estimated hysteresis loop using the Voigt model. The hysteresis loop depicted using the estimated parameters was close to that obtained after correction using the propagation time, which shows the effectiveness of the proposed method.

Figure 9 shows the transient change in the arterial diameter measured during FMD in three subjects. In all subjects, the diameter increased more than 10% after avascularization.

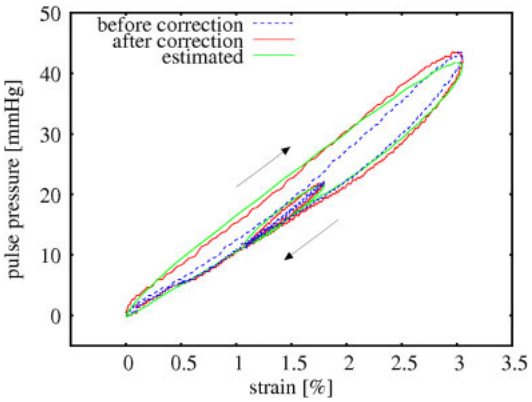

Fig. 8. (Color online) Measured hysteresis loops before and after correction of the propagation time and estimated hysteresis loop in in vivo measurement.

Because the increase in the diameter of healthy people is more than 6%, this result is consistent with previous reports.

Figures 10 and 11 respectively show the transient changes in the estimated stiffness parameter β and viscosity parameter of the radial artery wall during FMD reaction. In all three subjects, the stiffness parameter β temporarily decreased after avascularization. The variance of the viscosity parameter was smaller than that in the previous study,[18] showing the robustness of the proposed compensation method. The small variance may be due to the estimation of arterial diameter compared with that of artery wall thickness.

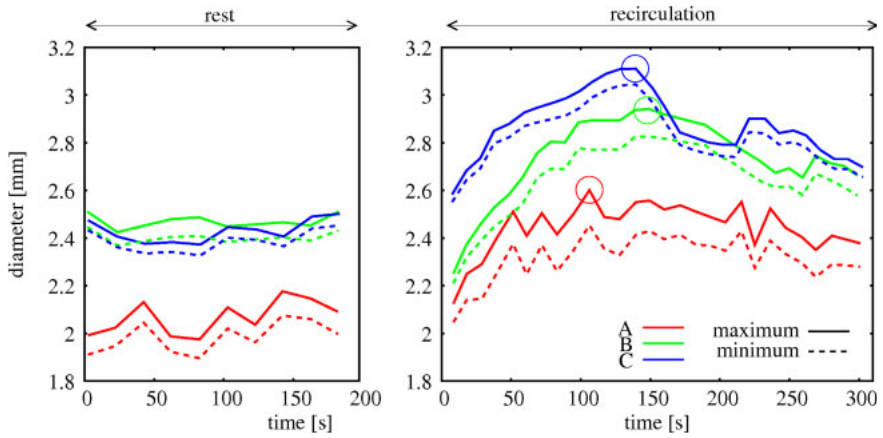

Fig. 9. (Color online) Transient change in the diameter during FMD for three healthy subjects (circles: the time showing the maximum diameter).

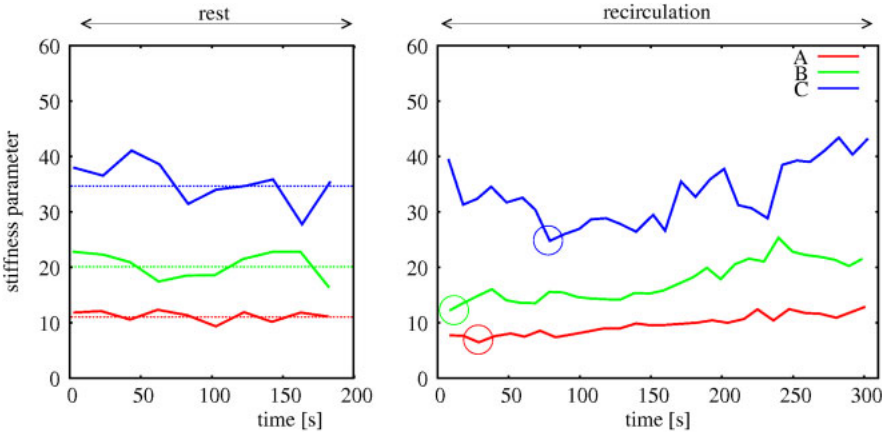

Fig. 10. (Color online) Transient change in the stiffness parameter β during FMD reaction for 3 healthy subjects (dotted lines: the mean during rest, circles: the time showing the smallest stiffness parameter).

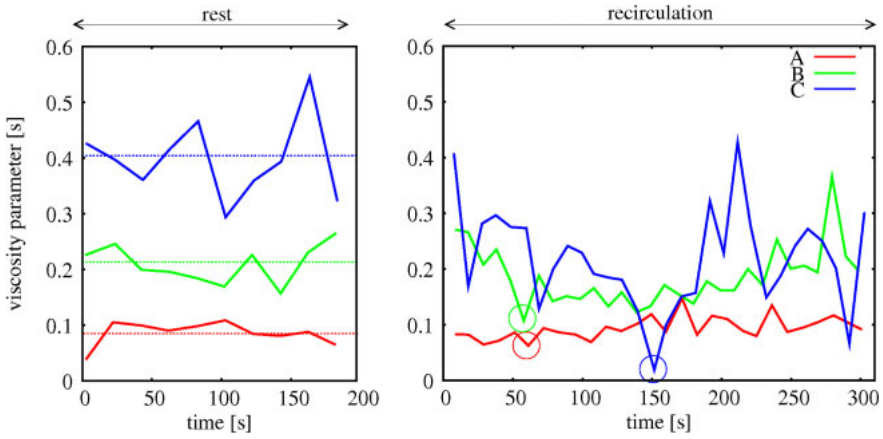

Fig. 11. (Color online) Transient change in the viscosity parameter during FMD reaction for 3 healthy subjects (dotted lines: the mean during rest, circles: the time showing the smallest viscosity parameter).

Figure 12 shows the measured relationship between diameter and pressure during the FMD reaction for subject A. The slope of the hysteresis loop, which corresponds to the stiffness parameter β, decreased after avascularization. These results validate the accuracy of the proposed method.

4. Discussion

In the experiment using a phantom, the incremental elasticity estimated by the proposed method was close to that measured by a tensile tester, the difference being about 1.9% of the value estimated by the proposed method. However, the difference in incremental viscosity was 30.3%. This large difference may have been caused by the difference in strain rate between the experiment using the proposed method and the tensile test. Because the viscosity is generally largely dependent on the strain rate, it is necessary to use the same strain rate in order to evaluate the estimation accuracy of the viscosity. The maximum strain rate of the phantom was about 0.18%/s in the ultrasound measurement. However, the upper limit of the strain rate was 0.15%/s in the tensile test, and it

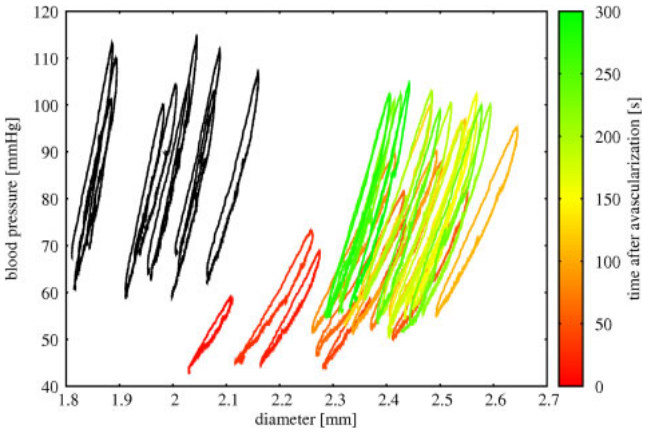

Fig. 12. (Color online) Measured relationship between diameter and pressure during FMD for subject A.

was not possible to use the same strain rate for both measurements.

The pulse pressure estimated by the proposed method largely decreased just after avascularization, as shown in Fig. 7. The decrease in arterial blood pressure may have been caused by the stoppage of blood circulation, because blood circulation maintains the difference between arterial and venous blood pressures. During avascularization, arterial blood pressure decreases and venous blood pressure increases. Since the arterial blood pressure did not recover immediately, this may have caused the low pulse pressure just after avascularization.

Within 50 s after avascularization, the arterial wall softened; however, the arterial diameter was not large enough compared with that at rest because of the low systolic blood pressure, as shown in Figs. 7, 9, and 10. From 50 to 150 s after avascularization, the arterial diameter increased as the systolic blood pressure increased, and the diameter had the maximum value from 100 to 150 s after avascularization. This result indicates that a conventional FMD measurement does not consider the decrease in systolic blood pressure, and the conventional measurement will work from 50 to 150 s after avascularization, that is, after the recovery of systolic blood pressure.

The proposed method considers the decrease in systolic blood pressure in estimating the stiffness parameter β. As shown in Fig. 10, within 100 s after avascularization, the stiffness parameter β estimated by the proposed method decreased, that is, the arterial wall softened by the FMD reaction. This result indicates the high performance of the proposed method in evaluating vascular endothelial function just after avascularization, where the function is difficult to be estimated by a conventional FMD measurement.

5. Conclusions

In the present study, we proposed a method of estimating viscoelasticity that uses two pressure sensors for arterial pressure measurement and a commercial ultrasound diagnostic device with a 7.5 MHz probe for arterial diameter measurement at the same position. We evaluated the accuracy of the estimation of viscoelasticity by the proposed method in a phantom experiment. The obtained results showed the accuracy of the reproducibility of the proposed method. In addition, arterial diameters and viscoelasticity during FMD reaction were measured in three healthy subjects. The proposed method revealed the softening of the arterial wall due to the FMD reaction within 100 s after avascularization. This result indicates the high performance of the proposed method in evaluating vascular endothelial function just after avascularization, where the function is difficult to be estimated by a conventional FMD measurement.

1) E. Wetter and T. Kenner, *Grundlagen der Dynamik des Arterienpulses* (Springer, Berlin, 1968) p. 379 [in German].
2) D. A. McDonald, *Blood Flow in Arteries* (Edward Arnold, London, 1974) 2nd ed., p. 284.
3) J. I. Weitz, X. Chair, J. Byrne, G. Patrick Clagett, M. E. Farkouh, J. M. Porter, D. L. Sackett, D. E. Strandness, Jr., and L. M. Taylor, Circulation **94**, 3026 (1996).
4) R. Ross, New Engl. J. Med. **340**, 115 (1999).
5) K. Node, Nikkei Medical Express (May, 2013) [in Japanese].
6) H. Iwasaki, M. Shichiri, F. Marumo, and Y. Hirata, Endocrinology **142**, 564 (2001).
7) R. F. Furchgott, Circ. Res. **53**, 557 (1983).
8) M. C. Corretti, T. J. Anderson, E. J. Benjamin, D. Celermajer, F. Charbonneau, M. A. Creager, J. Deanfield, H. Drexler, M. Gerhard-Herman, D. Herrington, P. Vallance, J. Vita, and R. Vogel, J. Am. Coll. Cardiol. **39**, 257 (2002).
9) N. M. AbdelMaboud and H. H. Elsaid, Egypt. J. Radiat. Nucl. Med. **44**, 237 (2013).
10) T. Nakamura, Y. Kitta, M. Uematsu, W. Sugamata, M. Hirano, D. Fujioka, K. Sano, Y. Saito, K. Kawabata, J. Obata, and K. Kugiyama, Int. J. Cardiol. **167**, 555 (2013).
11) C. D. Black, B. Vickerson, and K. K. McCully, Dyn. Med. **2**, 1 (2003).
12) Ø. Rognmo, T. H. Bjørstad, C. Kahrs, A. E. Tjønna, A. Bye, P. M. Haram, T. Stølen, S. A. Slørdahl, and U. Wisløff, J. Strength Cond. Assoc. **22**, 535 (2008).
13) T. Kaneko, H. Hasegawa, and H. Kanai, Jpn. J. Appl. Phys. **46**, 4881 (2007).
14) K. Ikeshita, H. Hasegawa, and H. Kanai, Jpn. J. Appl. Phys. **47**, 4165 (2008).
15) K. Ikeshita, H. Hasegawa, and H. Kanai, Jpn. J. Appl. Phys. **48**, 07GJ10 (2009).
16) K. Ikeshita, H. Hasegawa, and H. Kanai, Jpn. J. Appl. Phys. **50**, 07HF08 (2011).
17) K. Ikeshita, H. Hasegawa, and H. Kanai, Jpn. J. Appl. Phys. **51**, 07GF14 (2012).
18) M. Sato, H. Hasegawa, and H. Kanai, Jpn. J. Appl. Phys. **53**, 07KF03 (2014).
19) Z. Qu and Y. Ono, Jpn. J. Appl. Phys. **54**, 07HF01 (2015).
20) R. Nagaoka, R. Iwasaki, M. Arakawa, K. Kobayashi, S. Yoshizawa, S. Umemura, and Y. Saijo, Jpn. J. Appl. Phys. **54**, 07HF08 (2015).
21) R. K. Parajuli, N. Sunaguchi, R. Tei, T. Iijima, and Y. Yamakoshi, Jpn. J. Appl. Phys. **53**, 07KF30 (2014).
22) T. Shiina, Jpn. J. Appl. Phys. **53**, 07KA02 (2014).
23) Y. Fujita, H. Tagashira, H. Hasegawa, K. Fukunaga, and H. Kanai, Jpn. J. Appl. Phys. **53**, 07KF25 (2014).
24) H. Kanai, M. Sato, Y. Koiwa, and N. Chubachi, IEEE Trans. Ultrason. Ferroelectr. Freq. Control **43**, 791 (1996).
25) K. Nakahara, H. Hasegawa, and H. Kanai, Jpn. J. Appl. Phys. **53**, 07KF09 (2014).
26) K. Tachi, H. Hasegawa, and H. Kanai, Jpn. J. Appl. Phys. **53**, 07KF17 (2014).
27) Y. Nagai, H. Hasegawa, and H. Kanai, Jpn. J. Appl. Phys. **53**, 07KF19 (2014).
28) J. Alastruey, A. W. Khir, K. S. Matthys, P. Segers, S. J. Sherwin, P. R. Verdonck, K. H. Parker, and J. Peiro, J. Biomech. **44**, 2250 (2011).
29) K. Niki, M. Sugawara, D. Chang, A. Harada, T. Okada, R. Sakai, K. Uchida, R. Tanaka, and C. E. Mumford, Heart Vessels **17**, 12 (2002).
30) Y. Miyachi, H. Hasegawa, and H. Kanai, Jpn. J. Appl. Phys. **54**, 07HF18 (2015).